

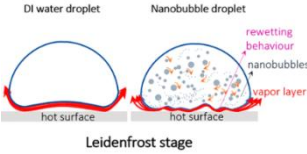
Sl. No.	<p style="text-align: center;">IIT Ropar List of Recent Publications with Abstract Coverage: December, 2022</p>
1.	<p>3D printing with biomaterials: A prospective view for biomedical applications R Kumar, H Singh, AK Sahani, P Sarkar - <i>Innovative Processes and Materials in Additive Manufacturing: Book Chapter, 2022</i></p> <p>Abstract: Manufacturing is the backbone of the economy as this ensures the incoming and outgoing of the raw materials and the finished products in the market, creating various employment opportunities. The complexity in design and production along with the ease of manufacturing is the main focus of concern as per the current trends. Additive manufacturing (AM) is a boon for the industries as it can produce complex shapes with ease that are not easy to produce with manual subtractive methods. The basic manufacturing procedure in the AM process is the designing of the product using the CAD tools which further is converted to the specific format (like .stl) files that usually contain the information in the sliced form, readable by the machine. 3D printers print the product using various printing techniques having different states of starting material. Generally, printers are classified into four categories according to their starting materials like solid filament, liquid, paste, and powder. Nowadays, bio-inks are popular and used in tissue, cell, and organ printing. The manual culturing of cells and tissue is a very cumbersome and time-consuming process and if any contamination gets incorporated, it may deteriorate the whole process. 3D printers are therefore potential candidates for printing bio-organ safely. This chapter describes various biomaterials that are used in 3D bioprinting for various biomedical applications.</p>
2.	<p>A compact 3-D multisector orientation insensitive wireless power transfer system M Kumar, S Kumar, A Sharma - <i>IEEE Microwave and Wireless Components Letters, 2022</i></p> <p>Abstract: The power conversion efficiency (PCE) in wireless power transfer (WPT) degrades due to angular misalignment between the transmitter (Tx) and the rectenna (Rx) along the azimuth plane. Therefore, a compact 3-D multisector orientation insensitive WPT system is proposed to address this problem. The optimal number of sectors () is determined analytically using patch antenna design equations to mitigate the effects of angular misalignment. In addition, conditions on the receiver antenna radiation pattern are investigated to enhance the performance of the WPT system. Furthermore, the observed conditions are utilized for designing a high gain WPT system at GHz with sectors. The proposed WPT system provides uniform power harvesting capability in the azimuth plane and higher power harvesting capacity than the patch antenna WPT system</p>
3.	<p>A comprehensive review and analysis of Masing/non-Masing behavior of materials under fatigue SS Yadav, SC Roy, S Goyal - <i>Fatigue & Fracture of Engineering Materials & Structures, 2022</i></p> <p>Abstract: Over the last 50 years, many researchers have contributed significantly towards understanding the Masing/non-Masing behavior of materials. However, there has been no review article or scientific report published to date that highlights the progress made in this domain. This article presents a state-of-the-art comprehensive review and analysis of the Masing/non-Masing behavior of materials under low cycle fatigue loading. Understanding of Masing/non-Masing behavior is important for the development of fatigue-resistant materials, prediction of fatigue life, and constitutive modeling and simulation. The influence of various factors such as stacking fault energy, temperature, strain amplitude, and loading conditions on Masing/non-Masing behavior has been summarized in this article. The literature pertaining to the internal microstructural changes observed in different materials by various researchers has been collected and compiled. The different methods of analyzing Masing/non-Masing behavior reported in the open literature are assessed and presented. The importance/significance of Masing/non-Masing</p>

	<p>behavior in constitutive modeling and fatigue life prediction has also been highlighted. Finally, conclusions based on the review and the potential problems required to be resolved in the future are also pointed out.</p>
4.	<p>A modified approach to determine mean sediment load and related discharge indices for suspended sediment transport S Maheshwari, SR Chavan - Journal of Hydrology, 2022</p> <p>Abstract: Discharge indices, viz., half-load discharge ($Q_{1/2}$), and functional-equivalent discharge (Q_{fed}), can be used to quantify the effectiveness of flow distribution in sediment transport through a river network. $Q_{1/2}$ represents the flow below and above which half of the total long-term sediment load is transported, while Q_{fed} indicates a uniform flow that replicates the total magnitude of the sediment load transported by the complete discharge distribution. In Magnitude Frequency Analysis (MFA), these indices are computed based on the estimate of mean sediment load (μS) transported through a river network. Conventionally, the analytical expression for μS was derived by assuming the discharges to be lognormally (LN) or Gamma (G) distributed. However, the assumption of discharge distribution is location specific and hence LN or G distributed discharge may not be valid for all catchments. Thus, it is necessary to assess the uncertainty in the estimate of μS and thereby the estimates of $Q_{1/2}$ and Q_{fed} when the discharge data do not follow either LN or G distribution. In this study, a modified approach is proposed to determine μS and related $Q_{1/2}$ and Q_{fed} for the general distribution of discharge datasets. The Proposed Approach (PA) includes the transformation of discharge data by applying the Box-Cox transformation followed by the estimation of μS, $Q_{1/2}$, and Q_{fed}. Furthermore, an analytical expression is derived for the solution of μS under the proposed framework. A simulation experiment is performed to establish the effectiveness of PA over the conventional (LN or G-based) approaches. Results indicated that PA provides reliable estimates of μS, $Q_{1/2}$, and Q_{fed}. The utility of the PA is demonstrated through its application to suspended sediment transport in four South Indian rivers.</p>
5.	<p>A multi-threading algorithm for constrained path optimization problem on road networks KK Dutta, A Dewan, VMV Gunturi - Web Information Systems Engineering: Lecture Notes in Computer Science, 2022</p> <p>Abstract: The constrained path optimization (CPO) problem takes the following input: (a) a road network represented as a directed graph, where each edge is associated with a “cost” and a “score” value; (b) a source-destination pair and; (c) a budget value, which denotes the maximum permissible cost of the solution. Given the input, the goal is to determine a path from source to destination, which maximizes the “score” while constraining the total “cost” of the path to be within the given budget value. CPO problem has applications in urban navigation. However, the CPO problem is computationally challenging as it can be reduced to an instance of the arc orienteering problem, which is known to be NP-hard. Given its heavy computational nature, the current state-of-the-art algorithms for this problem explore only a limited amount of search space to come up with a solution within a reasonable amount of execution time (around a few seconds). As a result, these algorithms often miss out on promising candidates and thus, result in low solution quality. In contrast, this paper proposes a novel algorithm called <i>Parallel-Spatial-RG</i>, which explores a much larger search space and obtains a significantly better solution quality. By using multiple threads, <i>Parallel-Spatial-RG</i> keeps the execution time within feasible limits by smartly distributing the total workload evenly among all the available threads. Moreover, <i>Parallel-Spatial-RG</i> is also able to demonstrate an almost linear speed-up with an increase in the number of cores.</p>
6.	<p>A planar integrated rectenna array with 3D-spherical DC coverage for orientation-tolerant wireless power transfer enabled IoT sensor nodes M Kumar, S Kumar, A Bhaduria, A Sharma - IEEE Transactions on Antennas and Propagation, 2022</p>

	<p>Abstract: Multiple IoT sensor nodes with RF power harvesting are deployed in random positions and orientations with respect to the power transmitter (Tx) generally installed on ceiling and side walls. The IoT sensor nodes with wireless power transfer (WPT) systems employing conventional rectenna designs with complex structures can provide only 2D coverage, thus, free-positioning and orientation-insensitive WPT is unrealizable. Therefore, a novel, compact, planar-integrated rectenna-array providing 3D-spherical coverage is proposed for the WPT system in 2-layer PCB technology. The proposed design scheme harvests maximum RF power in both, azimuth and elevation planes, by encapsulating end-fire and inherent tilted-beam bore-sight rectenna elements within a single sector. The radial integration of six such sectors coordinately achieves 3D-spherical DC coverage, and the bore-sight 3×1 patch antenna array functions as a dc low pass filter offering miniaturization and insertion loss reduction. The end-fire and bore-sight rectenna components harvest 240 mV and 255 mV at 1280Ω and 1176Ω output loads with RF-DC conversion efficiency of 69.1 % and 65.28 % at 5.8 GHz, respectively. Further, the rectenna elements are integrated using a simple and easily realizable low-loss parallel dc combining circuit, making it suitable for IoT sensor nodes.</p>
7.	<p>A switched modular multi-coil array transmitter pad with coil rectenna sensors to improve lateral misalignment tolerance in wireless power charging of drone systems A Bharadwaj, A Sharma, CC Reddy - IEEE Transactions on Intelligent Transportation Systems, 2022</p> <p>Abstract: In this article, a Switched Modular Multi-coil Array transmitter pad integrated with coil RecTenna (SMMART) is designed to present an intelligent wireless drone charging system that improves lateral misalignment tolerance. The resultant optimized design constitutes four independent transmitter modules, wherein each includes four spatially distributed 2×2 array coils. Therefore, the proposed design induces a maximal uniform voltage in the Rx coil region. Moreover, the optimization procedure accounts for the miniaturization of transmitter coil size without compromising the misalignment tolerance by overlapping various transmitter modules. In addition, a novel coil-based detection system for wireless chargeable drone applications is proposed to activate the desired transmitter module based on the position of the receiver coil. The detection system consists of an array of coil rectennas integrated with a switching circuit to reduce the undesired magnetic field, enhancing the link efficiency. The prototype of the charging pad is fabricated using Litz wire, and the S21-based link efficiency is measured using an experimental setup. Besides, the fabricated coil rectenna sensor array system demonstrates a real-application model of the detection system. Hence, the proposed transmitter pad improves lateral misalignment tolerance and is considered a potential wireless drone charging system design.</p>
8.	<p>A transfer learning approach to expedite training of artificial neural networks for variability-aware signal integrity analysis of MWCNT interconnects S Guglani, K Dimple, A Dasgupta, R Sharma... - IEEE 31st Conference on Electrical Performance of Electronic Packaging and Systems (EPEPS), 2022</p> <p>Abstract: In this paper, an artificial neural network (ANN) trained using a novel transfer learning approach is presented for the variability-aware signal integrity analysis of on-chip multi-walled carbon nanotube (MWCNT) interconnects. In the proposed transfer learning approach, initially a secondary ANN is trained to emulate the signal integrity quantities of interest of an approximate equivalent single conductor (ESC) model of the MWCNT interconnects. Thereafter, the values of the weights and bias terms of this secondary ANN are used to expedite the training of the primary ANN that will emulate the signal integrity quantities of the more rigorous multiconductor circuit (MCC) model of the MWCNT interconnects.</p>
9.	<p>Abrupt pattern transitions in argon ion bombarded swinging Si substrates Rakhi, S Sarkar - Physical Review B, 2022</p>

	<p>Abstract: We investigated morphology evolution of 500-eV Ar⁺ sputtered Si surfaces at an incidence of 67° using an unconventional method of substrate swinging by different azimuthal angles ($\Delta\phi$ from 0°→360°) and speeds up to 16 rotations per minute (RPM). The samples displayed four different regimes when they were swung azimuthally by different angles at a speed of 1 RPM. Initially, a hierarchical structure (regime 1) comprised of ripples and triangles was obtained which gave way to only ripples (regime 2) at $\Delta\phi=80^\circ$. A narrow third regime showed a completely flat surface at 100°. Above this angle, only disordered ripples devoid of any triangles were obtained up to 360° (regime 4). This regime also demonstrated drastic changes in orientation of the ripple wave vector at certain angles of $\Delta\phi$. The wavelengths and roughnesses decreased with higher azimuthal angles. Our observations were found to be highly reproducible. Upon swinging the samples for $\Delta\phi=70^\circ$ at higher speeds resulted in disordered ripple structures with smoother surfaces. Ripples were found to be the most ordered for 1 RPM speed. In contrast to the above, samples rotated continuously for different durations, when compared with a static case, displayed isotropically roughened surfaces. Two-dimensional slope distributions of the morphologies demonstrated formation of asymmetric ripple structures on the surfaces. Our results were explained in the light of linear and nonlinear regimes of sputtering. The crucial role played by dispersive linear terms explained the formation of the hierarchical structures at small swing angles. Once the dispersive effects die down, the ripples change their orientation. The asymmetry in surface structures was explained by the near-surface mass transport phenomenon at oblique azimuthal angles. This study demonstrates the role of this unconventional technique to drive a system towards abrupt morphological transitions not observed otherwise.</p>
10.	<p>Algebraic method for approximate solution of scattering of surface waves by thin vertical barrier over a stepped bottom topography N Kumar, D Goyal, SC Martha - Contemporary Mathematics, 2022</p> <p>Abstract: A study on interaction of surface water waves by thin vertical rigid barrier over a step type bottom topography is analysed. The associated mixed boundary value problem is solved using the eigenfunction expansion of the velocity potential. The resulting system of equations, avoiding the traditional approach of employing application of orthogonality relations, is solved using algebraic least squares method giving rise the numerical values of the reflection and transmission coefficients by the barrier over step. The energy balance relation for the given problem is derived and verified numerically ensuring the correctness of the present results. The present results are also compared with the data available in the literature for the validation purpose. The effect of step height, length of the barrier and angle of incidence on the reflection coefficient and the non-dimensional horizontal force on the barrier have been investigated through different plots. It is observed that barrier along with step works as an effective barrier to reflect more incident waves causing calm zone along the leeside.</p>
11.	<p>An analytical framework of multisector rectenna array design for angular misalignment tolerant rf power transfer systems M Kumar, S Kumar, A Sharma - IEEE Transactions on Microwave Theory and Techniques, 2022</p> <p>Abstract: A design procedure is presented for an angular misalignment-tolerant multisector rectenna array used as a wireless energy harvesting (WEH) system. The proposed analytical framework derives constraints on the synthesized harvested dc power pattern of the rectenna element as a solution to completely mitigate the angular misalignment. The derived constraints determine the optimal number of sectors required to ensure uniform harvesting capability across the entire azimuth plane. This is analytically verified for a conventional patch antenna used in the rectenna element of the multisector WEH system. The design constraints give N=8 and 12 sectors the optimal solution for single patch and 2 × 1 patch array rectenna. Furthermore, a new</p>

	<p>multilayer wide-beam rectenna is proposed at 5.8 GHz requiring $N=6$ sectors to mitigate the angular misalignment with 36.5% size reduction when compared with the conventional patch WEH system. The prototype of the WEH systems using the conventional patch rectenna and the proposed rectenna is fabricated and measured. The measurement results corroborate the analytical and simulation results validating the capability of the proposed framework to achieve uniform energy harvesting in the entire azimuth plane.</p>
12.	<p>An approach in selective harmonic mitigation technique for reduction of multiple harmonics with only two switchings per quarter P Kalkal, AVR Teja - 48th Annual Conference of the IEEE Industrial Electronics Society, 2022</p> <p>Abstract: The selective harmonic elimination technique allows us to eliminate completely N number of harmonics with $(N+1)$ number of switchings per quarter. However, instead of completely removing grid regulations demand that harmonics be kept to less than 5%. Therefore, there exists a possibility of bringing more harmonics within the 5% band while keeping the number of switchings fixed. This degree of freedom is explored in this paper wherein many harmonics are mitigated while keeping only two switchings per quarter. The analysis is tested in simulation for various operating conditions using MATLAB/Simulink software. It is shown that up to 17th harmonic can be mitigated to less than 5% with two switchings per quarter.</p>
13.	<p>Analysis of thermal characteristics of batch cooling sonocrystallization: Effect on crystal attributes J Yadav, A Srivastava, SA Patel - Crystal Research and Technology, 2022</p> <p>Abstract: The control of desired product quality attributes in the crystallization process is one of the major concerns of the pharmaceutical industries due to the established standard limits for active pharmaceutical ingredients in applications. The objective of the present work is to establish the fundamental understanding and methodology of the batch cooling sonocrystallization process to tune the crystal attributes over the range of operating parameters, i.e., ultrasound amplitude, duration of sonication, and cooling rate. For the constant cooling rate, the effect of three levels of ultrasound amplitude has been investigated over the range of durations of insonation. It is observed for a fixed cooling rate that the optimized set of ultrasound parameters shortens the induction time resulting in a finer range of particles increasing the surface area and narrowing the particle size distribution. The performance of the process in terms of thermal characteristics has been analyzed to delineate the effect of operating parameters to be employed as a function of the product characteristics. The simple expressions for temperature profiles during the process have been proposed as a function of saturation temperature to facilitate their applications in the optimization of the operating parameters for the desired product size and size range.</p>
14.	<p>Asymptotic analysis of elastic coupling in anisotropic-homogeneous beam N Shakya, SS Padhee - Journal of Applied Mechanics, 2022</p> <p>Abstract: Elastic coupling is extensively used for passive control of modern structures. This design philosophy has been extensively explored in composite beams, which are inherently inhomogeneous and anisotropic. Such in-depth investigation is not available for homogeneous-anisotropic beams. This paper investigates elastic coupling in homogeneous-anisotropic beam with elliptical cross section using variational asymptotic method (VAM). It is observed that the mere introduction of anisotropy does not couple the system completely. The coupling is tuneable and tailorable, depending on the material properties, their spatial distribution (homogeneity/inhomogeneity), and the geometrical parameters of the beam.</p>
15.	<p>Augmenting the leidenfrost temperature of droplets via nanobubble dispersion GVVS Vara Prasad, H Sharma, N Nirmalkar, P Dhar, D Samanta - Langmuir, 2022</p> <p>Abstract: Droplets may rebound/levitate when deposited over a hot substrate (beyond a critical</p>

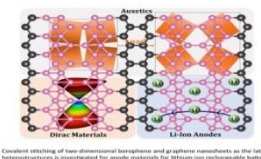
	<p>temperature) due to the formation of a stable vapor microcushion between the droplet and the substrate. This is known as the Leidenfrost phenomenon. In this article, we experimentally allow droplets to impact the hot surface with a certain velocity, and the temperature at which droplets show the onset of rebound with minimal spraying is known as the dynamic Leidenfrost temperature (T_{DL}). Here we propose and validate a novel paradigm of augmenting the T_{DL} by employing droplets with stable nanobubbles dispersed in the fluid. In this first-of-its-kind report, we show that the T_{DL} can be delayed significantly by the aid of nanobubble-dispersed droplets. We explore the influence of the impact Weber number (We), the Ohnesorge number (Oh), and the role of nanobubble concentration on the T_{DL}. At a fixed impact velocity, the T_{DL} was noted to increase with the increase in nanobubble concentration and decrease with an increase in impact velocity for a particular nanobubble concentration. Finally, we elucidated the overall boiling behaviors of nanobubble-dispersed fluid droplets with the substrate temperature in the range of 150–400 °C against varied impact We through a detailed phase map. These findings may be useful for further exploration of the use of nanobubble-dispersed fluids in high heat flux and high-temperature-related problems and devices.</p>  <p style="text-align: center;">Leidenfrost stage</p>
16.	<p>Behind the scenes of a postgraduate curriculum design in an autonomous institute N Goel, SS Jha, SRS Iyenger - Proceedings of the 15th Annual ACM India Compute Conference, 2022</p> <p>Abstract: Post graduate (PG) programs in computer science provide domain specialization to the students. These PG programs also serve as prerequisites for doctoral programs at various universities. This article discusses various factors that impact the designing of a PG curriculum from scratch. We propose an approach that considers the objectives of the program, curricula reports of ACM, other model curricula, and the technical background of students. Based on the standard approaches and requirements, we hand-crafted our curriculum for the PG program in computer science. We show the effectiveness of the proposed curriculum with qualitative analyses.</p>
17.	<p>Boundedness of composition operator on several variable Paley-Wiener space A Samanta, S Sarkar - Linear Algebra and its Applications, 2023</p> <p>Abstract: In this paper we have considered composition operators on the several variable Paley-Wiener space $L^2_\pi(\mathbb{C}^n)$. We have proved that for any continuous function $\varphi : \mathbb{C}^n \rightarrow \mathbb{C}^n$ the composition operator C_φ on $L^2_\pi(\mathbb{C}^n)$ is bounded iff φ has the following form: $\varphi(z) = Az + b, z \in \mathbb{C}^n$, where $A \in GL(n, \mathbb{R})$ with $\ A\ _{op} \leq 1$ and $b \in \mathbb{C}^n$. Our proof is different from the single variable case and mainly depends on a theorem of Malgrange, some techniques from harmonic analysis and certain asymptotic behaviour of Bessel's function.</p>
18.	<p>Can natural products targeting emt serve as the future anticancer therapeutics? S Anwar, JA Malik... - Molecules, 2022</p> <p>Abstract: Cancer is the leading cause of death and has remained a big challenge for the scientific community. Because of the growing concerns, new therapeutic regimens are highly demanded to decrease the global burden. Despite advancements in chemotherapy, drug resistance is still a major hurdle to successful treatment. The primary challenge should be identifying and developing appropriate therapeutics for cancer patients to improve their survival.</p>

	<p>Multiple pathways are dysregulated in cancers, including disturbance in cellular metabolism, cell cycle, apoptosis, or epigenetic alterations. Over the last two decades, natural products have been a major research interest due to their therapeutic potential in various ailments. Natural compounds seem to be an alternative option for cancer management. Natural substances derived from plants and marine sources have been shown to have anti-cancer activity in preclinical settings. They might be proved as a sword to kill cancerous cells. The present review attempted to consolidate the available information on natural compounds derived from plants and marine sources and their anti-cancer potential underlying EMT mechanisms.</p>
<p>19.</p>	<p>Collaborative dispersion by silent robots B Gorain, PS Mandal, K Mondal, S Pandit - Stabilization, Safety, and Security of Distributed Systems: Lecture Notes in Computer Science, 2022</p> <p>Abstract: In the dispersion problem, a set of k co-located mobile robots must relocate themselves in distinct nodes of an unknown network. The network is modeled as an anonymous graph $G=(V,E)$, where the graph's nodes are not labeled. The edges incident to a node v with degree d are labeled with port numbers in the range $\{0,1,\dots,d-1\}$ at v. The robots have unique IDs in the range $[0, L]$, where $L \geq k$, and are initially placed at a source node s. Each robot knows only its ID, however, it does not know the IDs of the other robots or the values of L or k. The task of the dispersion was traditionally achieved based on the assumption of two types of communication abilities: (a) when some robots are at the same node, they can communicate by exchanging messages between them, and (b) any two robots in the network can exchange messages between them.</p> <p>This paper investigates whether this communication ability among co-located robots is absolutely necessary to achieve the dispersion. We established that even in the absence of the ability of communication, the task of the dispersion by a set of mobile robots can be achieved in a much weaker model, where a robot at a node v has the access of following very restricted information at the beginning of any round: (1) am I alone at v? (2) did the number of robots at v increase or decrease compared to the previous round?</p> <p>We propose a deterministic distributed algorithm that achieves the dispersion on any given graph $G=(V,E)$ in time $O(k \log L + k^2 \log \Delta)$, where Δ is the maximum degree of a node in G. Further, each robot uses $O(\log L + \log \Delta)$ additional memory. We also prove that the task of the dispersion cannot be achieved by a set of mobile robots with $o(\log L + \log \Delta)$ additional memory.</p>
<p>20.</p>	<p>Computationally Efficient Model Predictive Torque Control of Switched Reluctance Motor Drives K Jayasawal, AK Rana, AVR Teja - 48th Annual Conference of the IEEE Industrial Electronics Society, 2022</p> <p>Abstract: This paper proposes a computationally efficient Finite Control Set-Model Predictive Torque Control (FCS-MPTC) algorithm to reduce the torque ripple in switched reluctance motor (SRM) drives. The computational burden is minimized in two ways, one by using a single look-up table based technique for estimating the torque and the other by reducing the switching vectors to be evaluated at any instant to a maximum of three. The single LUT-based torque estimation is done using $k(\theta, i)$ profile that gives a non-linear modulating factor to be multiplied with the linear torque. Furthermore, a controlled demagnetization of the outgoing phase is realized during the magnetization of the incoming SRM phase for the entire overlapping region thereby reducing the torque ripple. The proposed model is verified through MATLAB/Simulink on a four-phase 8/6 SRM. Using the proposed method, a torque ripple of $\approx 6\%$ has been achieved.</p>

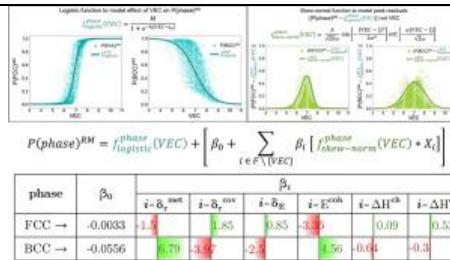
21.	<p>Consolidated adversarial network for video de-raining and de-hazing VM Galshetwar, A Kulkarni, S Chaudhary - IEEE International Conference on Advanced Video and Signal Based Surveillance, 2022</p> <p>Abstract: The performance of recent video enhancement methods is superior in specific hazy, rainy, snowy, and foggy weather conditions. However, these approaches can handle degradation rendered by single weather. We propose an integrated lightweight adversarial learning network to handle the degradations induced by different weather conditions. This is a unique approach to mitigate the problem of video restoration for multi- weather degraded videos using single network. The proposed architecture combines the idea of multi-resolution analysis with a multi-scale encoder and domain-specific feature learning is achieved using domain-aware filtering modules. The architecture provides recurrent feature sharing for temporal consistency, achieved by feeding the previous frame output as feedback. Substantial experiments on various datasets demonstrate that the proposed method performs competitively with the existing state-of-the-art approaches for video restoration in multi-weather conditions.</p>
22.	<p>Deep insights of learning based micro expression recognition: A perspective on promises, challenges and research needs M Verma, SK Vipparthi, G Singh - IEEE Transactions on Cognitive and Developmental Systems, 2022</p> <p>Abstract: Micro expression recognition (MER) is a very challenging area of research due to its intrinsic nature and fine-grained changes. In the literature, the problem of MER has been solved through handcrafted/descriptor-based techniques. However, in recent times, deep learning (DL) based techniques have been adopted to gain higher performance for MER. Also, rich survey articles on MER are available by summarizing the datasets, experimental settings, conventional and deep learning methods. In contrast, these studies lack the ability to convey the impact of network design paradigms and experimental setting strategies for DL based MER. Therefore, this paper aims to provide a deep insight into the DL-based MER frameworks with a perspective on promises in network model designing, experimental strategies, challenges, and research needs. Also, the detailed categorization of available MER frameworks is presented in various aspects of model design and technical characteristics. Moreover, an empirical analysis of the experimental and validation protocols adopted by MER methods is presented. The challenges mentioned earlier and network design strategies may assist the affective computing research community in forge ahead in MER research. Finally, we point out the future directions, research needs and draw our conclusions.</p>
23.	<p>Digital screening and brief intervention for illicit drug misuse in college students: A mixed methods, pilot, cluster, randomized trial from India K Sharma, A Ghosh, NC Krishnan, S Kathirvel, D Basu...A Kumar... - Asian Journal of Psychiatry, 2022</p> <p>Abstract: Background Adolescence and early adulthood are vulnerable periods for substance use-related disorders later in life. The use of internet-enabled interventions can be useful, especially in low-resource settings.</p> <p>Aims To examine the feasibility, acceptability, and preliminary effectiveness of single-session digital screening and brief intervention (d-SBI) for illicit drug misuse in college students and explore barriers and facilitators of d-SBI.</p> <p>Methods</p>

	<p>Design: Mixed-methods, pilot cluster randomized trial. Setting: Four conveniently selected colleges were randomized into intervention and control groups.</p> <p>Participants: 219 students were screened, and 37 fulfilled eligibility. Twenty-four completed follow-ups. In-depth interviews were done with ten students.</p> <p>Intervention and Comparator: Following a digital screening, Alcohol, Smoking, and Substance Involvement Screening Test (ASSIST) based brief intervention was provided in the d-SBI group. The control group received brief education.</p> <p>Measurements: Acceptability was assessed by direct questions and usage statistics. ASSIST scores of groups were assessed at baseline and 3 months. Inductive coding of the interview transcript was done.</p> <p>Results: More than 50 % of participants found d-SBI user-friendly, appropriate, and useful. Eighty percent of users, who logged in, completed screening. Per-protocol analysis showed a reduction in cannabis-ASSIST score over 3 months. The mean ASSIST score for other drugs combined did not differ significantly between groups. The difference in risk transition (moderate to low) was not significant. Qualitative analysis revealed three overarching themes- recruitment, engagement, and behavior change.</p> <p>Conclusions Digital SBI for drug misuse is feasible among college students. d-SBI might be effective in reducing cannabis use.</p>
24.	<p>Edge exploration of anonymous graph by mobile agent with external help AK Dhar, B Gorain, K Mondal, S Patra, RR Singh - Computing, 2022</p> <p>Abstract: Exploration of an unknown network by one or multiple mobile entities is a well studied problem which has various applications like treasure hunt, collecting data from some node in the network or samples from contaminated mines. In this paper, we study the problem of edge exploration of an n node graph by a mobile agent. The nodes of the graph are anonymous, and the edges at a node of degree d are arbitrarily assigned unique port numbers in the range $0, 1, \dots, d-1, \dots, d-1$. A mobile agent, starting from a node, has to visit all the edges of the graph and stop. The time of the exploration is the number of edges the agent traverses before it stops. The task of exploration can not be performed even for a class of cycles if no additional help is provided. We consider two different ways of providing additional help to the agent by an Oracle. In the first scenario, the nodes of the graph are provided some short labels by the Oracle. In the second scenario, some additional information, called advice, is provided to the agent in the form of a binary string. For the first scenario, we show that exploration can be done by providing constant size labels to the nodes of the graph. For the second scenario, we show that exploration can not be completed within time $o(n^3)$ regardless of the advice provided to the agent. We propose an upper bound result by designing an $O(n^3)$ algorithm with $O(n \log n)$ advice. We also show a lower bound $\Omega(n^3)$ on the size of advice to perform exploration in $O(n^3)$ time. In addition, we have done experimental studies on randomly created anonymous graph to analyze time complexity of exploration with $O(n \log n)$ size advice.</p>
25.	<p>Effect of corrosion location and transverse reinforcement on flexural-ductile response of reinforced concrete beams SN Amini, AS Rajput - International Journal of Civil Infrastructure (IJCI), 2022</p> <p>Abstract: Concern about premature ageing and deterioration of reinforced concrete (RC) structures primarily stems from reinforcement corrosion. The reinforcement corrosion not only reduces the effective cross-section of reinforcing bars but also causes a severe reduction in the structural performance and service life of RC structures. This study aims to analyze the effect of varying corrosion levels on the load-bearing ability of RC beams configured with varying amounts of transverse reinforcement. The idea pertinent to this study is to develop and validate a</p>

	<p>3D finite element numerical model of RC beams and subsequently simulate the corrosion deterioration to assess the effect of corrosion deterioration on the flexural response of RC beams. The beam models have been analyzed with a four-point simply supported bending flexural test. For concrete-steel interaction simulation, the cohesive surface interaction method proved to be most suitable as the results aligned well with the analytical results. Loss of bond in concrete-rebar interface due to decrease in mechanical interlock is calculated. The concrete Damage Plasticity model is adopted for calculating concrete's confined and unconfined strength in tension and compression. A parametric study is also performed to investigate varying corrosion percentages on residual capacity, stiffness, energy dissipation and behaviour of corroded beams. Flexural strength response due to spacing of transverse reinforcements as per different Indian standard codes is analyzed. Spalling stress is calculated analytically and used in simulation data for more precise results. The results indicate a notable reduction in load-deflection behaviour due to concrete spalling, deterioration of rebar ribs, loss in mechanical interlock mechanism and yield strength. The structure undergoes an absolute brittle failure at very high corrosion levels due to a complete steel-concrete bond loss. A good correlation between the developed FE model and experimental load-deflection curves was observed, with variability in ultimate load-bearing capacities of less than 5% for all the cases.</p>
26.	<p>Effective potentials in a rotating spin-orbit-coupled spin-1 spinor condensate P Banger, RK Kumar, A Roy, S Gautam - <i>Journal of Physics: Condensed Matter</i>, 2022</p> <p>Abstract: We theoretically study the stationary-state vortex lattice configurations of rotating spin-orbit (SO)- and coherently-coupled spin-1 Bose–Einstein condensates (BECs) trapped in quasi-two-dimensional harmonic potentials. The combined effects of rotation, SO and coherent couplings are analyzed systematically from the single-particle perspective. Through the single-particle Hamiltonian, which is exactly solvable for one-dimensional coupling, we illustrate that a boson in these rotating SO- and coherently-coupled condensates are subjected to effective toroidal, symmetric double-well, or asymmetric double-well potentials under specific coupling and rotation strengths. In the presence of mean-field interactions, using the coupled Gross–Pitaevskii formalism at moderate to high rotation frequencies, the analytically obtained effective potential minima and the numerically obtained coarse-grained density maxima position are in excellent agreement. On rapid rotation, we further find that the spin-expectation per particle of an antiferromagnetic spin-1 BEC approaches unity indicating a similarity in the response with ferromagnetic SO-coupled condensates.</p>
27.	<p>Eldfellite NaV(SO₄)₂ as a versatile cathode insertion host for Li-ion and Na-ion batteries S Singh, D Singh, R Ahuja... - <i>Journal of Materials Chemistry A</i>, 2022</p> <p>Abstract: In search of high energy density cathode materials, the eldfellite mineral-type NaV^{III}(SO₄)₂ compound has been theoretically predicted to be a promising cathode insertion host for sodium-ion batteries. Synergizing computational and experimental investigations, the current work introduces NaV^{III}(SO₄)₂ as a novel versatile cathode for Li-ion and Na-ion batteries. Prepared by a low temperature sol-gel synthesis route, the eldfellite NaV(SO₄)₂ cathode exhibited an initial capacity approaching ~79% (vs. Li⁺/Li) and ~69% (vs. Na⁺/Na) of the theoretical capacity (1e⁻ ≅ 101 mA h g⁻¹) involving the V³⁺/V²⁺ redox potential centered at 2.57 V and 2.28 V, respectively. The bond valence site energy (BVSE) approach and DFT-based calculations were used to gain mechanistic insight into alkali ion migration and probe the redox center during (de)insertion of Li⁺/Na⁺ ions. Post-mortem and electrochemical titration tools revealed the occurrence of a single-phase (solid-solution) redox mechanism during reversible Li⁺/Na⁺ (de)insertion into NaV^{III}(SO₄)₂. With the multivalent vanadium redox center, eldfellite NaV^{III}(SO₄)₂ forms a new cathode insertion host for Li/Na-ion batteries with potential two-electron uptake.</p>
28.	<p>Electrochemical sulfinylation of phenols with sulfides: a metal- and oxidant-free cross-coupling</p>

	<p>for the synthesis of aromatic sulfoxides R Kumar, IM Taily, P Banerjee - <i>Chemical Communications</i>, 2022</p> <p>Abstract: The site-selective C–H functionalization of arenes is of indisputable importance in organic chemistry. Herein, we have demonstrated an electrochemical regioselective oxidative cross-coupling towards the direct C(sp²)–H sulfinylation of phenols with sulfides under mild reaction conditions. The designed methodology furnished aryl sulfoxides in good to moderate yields under exogenous metal and oxidant-free conditions. Moreover, the exploitation of traceless electrons to carry out the tandem site-selective oxidative aryl chalcogenation is the striking feature of this methodology.</p>
29.	<p>Electronic level modelling of graphene-borophene lateral heterostructures as anodes in Li-ion batteries NVR Nulakani, TJD Kumar - <i>Applied Surface Science</i>, 2022</p> <p>Abstract: Covalent stitching of dissimilar semi-infinite two-dimensional (2D) nanosheets as the lateral heterostructures is relatively rare due to the various challenges involved in the experimental synthesis. In this study, we have integrated the graphene and borophene monolayers and created a series of lateral heterostructures inspired by their recent experimental synthesis. Further, we have systematically explored the geometrical, thermal, mechanical properties and electronic structure of these lateral heterostructures using the density functional theory calculations. Results authenticate that graphene and borophene lateral heterostructures (GBLHs) are dynamically and thermally stable. Further, they exhibit anisotropic mechanical properties including the negative Poisson's ratio. Electronic structure calculations reveal that the GBLHs can be classified as either semi-metals or metals and the conductivity depending on the width of the graphene and borophene chains comprises the heterostructure. Further, massless Dirac fermions and anisotropic high hole and electron mobilities are the prominent electronic features of the semi-metallic GBLHs. Finally, we have investigated the application potentials of GBLHs as the anode materials for lithium-ion rechargeable batteries (LIBs). Computed results illustrate that the GBLHs can serve as potential anode materials in the LIBs with intriguing features like metallicity, optimal adsorption energies, low diffusion barrier, enhanced specific storage capacity (1394.5 mA h g⁻¹) and an average open circuit voltage (~0.52 eV).</p> <p>Graphical Abstract:</p>  <p style="font-size: small; text-align: center;">Covalent stitching of two-dimensional borophene and graphene nanosheets as the lateral heterostructures is investigated for anode materials for lithium-ion rechargeable batteries.</p>
30.	<p>Emergence of considerable thermoelectric effect due to the addition of an underlayer in Pt/Co/Pt stack and its application in detecting field free magnetization switching R Posti, A Kumar, D Tiwari, D Roy - <i>Applied Physics Letters</i>, 2022</p> <p>Abstract: Application of sufficient lateral current to a heavy metal (HM) can switch the perpendicular magnetization orientation of an adjacent ferromagnetic layer through spin–orbit torques (SOTs). The choice of the HM and its arrangement plays a major role for the SOT induced magnetization switching in magnetic heterostructures. Generally, thin Ta is used as an underlayer to the HM layer for better adhesion and smoothness of the HM layer. Here, we show that Ta addition to the asymmetric stack Pt/Co/Pt gives rise to several compelling effects, viz., thermoelectric effects [particularly, anomalous Nernst effect (ANE)], and enhanced perpendicular magnetic anisotropy which was negligible in a Pt/Co/Pt stack. For this Ta/Pt/Co/Pt stack, the antidamping-SOT values are evaluated after carefully removing the contribution from</p>

	<p>the ANE and it is found to match the AD-SOT of the Pt/Co/Pt stack. We have observed current-induced field-free magnetization switching Ta/ Pt/Co/Pt stack with Co thickness gradient. Furthermore, we have utilized the thermoelectric effects to develop a technique to detect the fieldfree magnetization switching. This technique detects the second harmonic ANE signal as a reading mechanism. Using ANE symmetry with the applied current, the switching can be detected in a single current sweep which was corroborated to the conventional DC Hall method.</p>
31.	<p>Enhanced output power-density by sidelobe suppression of phase-locked lasers V Dev, ANK Reddy, V Pal - <i>Frontiers in Optics</i>, 2022</p> <p>Abstract: We present results on enhanced output power-density by sidelobe suppression of phase-locked lasers in various array geometries. The effect of system size, topological defects, and range of phase locking are studied.</p>
32.	<p>Falling ball method for determining zero shear and shear-dependent viscosity of polymeric systems: Solutions, melts, and composites P Suri, SA Patel, RP Chhabra - <i>Journal of Vinyl and Additive Technology</i>, 2022</p> <p>Abstract:The falling ball method (FBM) is one of the well-established techniques for measuring the viscosity of Newtonian liquids at the room as well as at elevated temperatures and pressures. Owing to its simplicity and low cost, the possibility of extending its range of application to non-Newtonian systems including virgin and filled polymer melts, composites, polymer-solutions, and so forth, is explored here, In this work, theoretical results for the flow of power-law fluids past a sphere have been used to extract the values of the zero-shear viscosity and shear-dependent viscosity in the low-shear rate limit. The theoretical scheme outlined here has been validated by presenting comparisons with experimental results for scores of polymer solutions for which both falling sphere and rheological data are available in the literature. Indeed, the good correspondence obtained between these two independent data is encouraging and it is thus possible to use the FBM for shear-thinning systems when the resulting Reynolds numbers are such that the flow is viscosity-dominated, and the inertial effects are negligible. This implies that the Reynolds number should be $\leq \sim 1$ for shear-thinning fluids and $\leq \sim 10^{-5}$ for shear-thickening fluids.</p>
33.	<p>FCC vs. BCC phase selection in high-entropy alloys via simplified and interpretable reduction of machine learning models D Beniwal, PK Ray – <i>Materialia</i>, 2022</p> <p>Abstract:Machine learning (ML) models for phase selection in high-entropy alloys often suffer from an inherent lack of interpretability despite remarkable advancements of late. Here we present a mathematical expression for the probability of occurrence of FCC and BCC phases in HEAs that was obtained through statistical analysis of the experimental data and ML models. The model presented here utilizes a logistic function to isolate the effect of valence electron count on FCC and BCC phase occurrence and models the residuals as a function of six other physical and thermodynamic descriptors. Thus, the complex ML model is replaced by a simplified and interpretable mathematical function. The proposed model is quite consistent with the ML model and experimental database and enables a direct quantitative estimation of feature contributions towards phase occurrence probabilities leading to insights into the decision-making process learnt by the ML model for phase selection in high-entropy alloys.</p> <p>Graphical Abstract:</p>



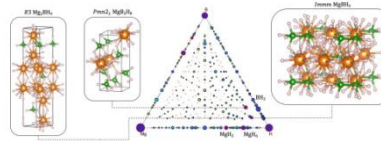
34.

[First-principles calculations on superconductivity and H-diffusion kinetics in Mg–B–H phases under pressures](#)

W Sukmas, P Tsuppayakorn-aek... R Ahuja... - International Journal of Hydrogen Energy, 2022

Abstract: Focusing towards ternary metal hydrides has recently been regarded as a new avenue for research in pressure-dependent high-temperature superconductors, thanks highly to a fairly large number of permutations of alloying metals, even metalloids, with hydrogen. Herein, new phases of Mg – B – H ternary hydrides are predicted from the first-principles evolutionary techniques, as a result of which the corresponding phonon and electronic calculations for the three candidate phases are performed successively to confirm their dynamic stability and the possibility to become conductors. The metallic MgBH₉ undergoes a superconducting phase with a maximum T_c of 64 K at 110 GPa, with its spectral function predominantly active around optical modes. The significant increase in cumulative electron-phonon coupling constant is associated with a relatively low cutoff frequency according to the bandwidth function. As for the non-metallic candidate, hydrogen-vacancy diffusion kinetics of the MgB₂H₈ phase are determined by means of total energy calculations. Stable pathways at varying pressure are reported, suggesting that elevated pressure lowers the activation energy which is presumably due to an optimal level of average nearest H – H(B) inter-fragment distances.

Graphical Abstract:



35.

[Four differential channels, programmable gain, programmable data rate delta sigma adc](#)
MA Saeed, D Sehgal, S Singh - International Symposium on VLSI Design and Test, 2022

Abstract: This paper presents a precision wide range Delta Sigma ADC SC1601 (SC1601 is the product number of ADC) with programmable gain amplifier (PGA) and programmable output data rate features. The ADC offers four fully differential input channels. Each channel can be programmed with a gain of 1 to 128 in binary steps i.e. in powers of 2. The ADC uses a second order delta sigma modulator (DSM) followed by a digital sinc33 filter. The output data rate of the ADC is also programmable from 312.5 Hz to 2.5 kHz either to achieve higher accuracy or higher speed. The ADC also offers on chip offset and gain calibration features to reduce the offset and gain errors. The serial interface of ADC is SPITMTM compatible. The SC1601 ADC is fabricated in 0.18 μm CMOS process at Semi-Conductor Laboratory (SCL). The total power consumption of the ADC is 4 mW and it consumes total silicon area of 2.25 mm². SC1601 ADC achieves a maximum ENOB of 19.15 bits at a data rate of 312.5 Hz with a full scale range of 1.22 V. The ADC requires a supply voltage of 3.3 V and 1.8 V and can operate in a wide temperature range of –55°C to 125°C. SC1601 ADC is developed for the satellite launch vehicle telemetry system.

36.

[Fusion-fission analysis of ¹²C + ²⁴⁸Cm and ¹⁶O + ²⁴⁴Pu nuclear reactions across the Coulomb barrier](#)

Vijay, N Grover, K Sharma, MS Gautam, MK Sharma... - Physical Review C, 2022

Abstract: By using the symmetric-asymmetric Gaussian barrier distribution (SAGBD) model, Wong formula, and coupled channel approach, heavy ion fusion dynamics is investigated for $^{12}\text{C}+^{248}\text{Cm}$ and $^{16}\text{O}+^{244}\text{Pu}$ reactions at energies lying below and near the Coulomb barrier. Coupling of various channels linked with the structure of participants to the relative motion of the collision partners is done by considering a Gaussian type of weight function in the SAGBD model and cross sections are found to be enhanced relative to the calculations obtained by the simple barrier penetration model. In the SAGBD model, the channel coupling effects are calculated in terms of channel coupling parameter (λ) and percentage reduction in the height of apparent fusion barrier with respect to the Coulomb barrier (VCBRED). The channel coupling parameter estimates the cumulative influence of dominant intrinsic channels, which are responsible for the sub-barrier fusion enhancement. The SAGBD calculations appropriately explain the dynamics of $^{12}\text{C}+^{248}\text{Cm}$ and $^{16}\text{O}+^{244}\text{Pu}$ reactions at energies lying around the Coulomb barrier. The coupled channel analysis of the present reactions is done by using the code ccfull and the coupled channel calculations unambiguously identify the dominant influences of the rotational states up to $10+$ spin states of the ground state rotational band of target isotopes in both reactions. In addition, the couplings to higher order deformation, such as β_4 for target and low lying quantum states of the projectile, are necessarily required to reproduce the experimental data of $^{12}\text{C}+^{248}\text{Cm}$ and $^{16}\text{O}+^{244}\text{Pu}$ reactions. Apart from the fusion analysis, the dynamical cluster-decay model (DCM) is applied to understand the fission dynamics of the $^{260}\text{No}^*$ nucleus formed via the above-mentioned reactions. The decay study is carried out at the center-of-mass energies spread, $E_{c.m.}$ (≈ 79 to 109 MeV) by including the quadrupole deformations (β_2) and optimum orientations (θ_{opti}) of the decaying fragments. According to the experimental observation, the noncompound nucleus (nCN) fission component competes with the compound nucleus (CN) fission processes. Consequently, the possibility of nCN contribution is also explored in the decay of the $^{260}\text{No}^*$ compound nucleus. With an aim to have a comprehensive analysis of CN and nCN fission mechanisms, the role of the center-of-mass energy ($E_{c.m.}$) and angular momentum (ℓ) is explored in terms of various parameters of DCM such as fragmentation potential, preformation probability, barrier modification, etc.

[Geographical concentration of knowledge and technology-intensive industries in India: empirical evidence from establishment-level analysis](#)

S Agarwal, SR Behera - Indian Economic Review, 2022

37.

Abstract: This paper investigates the geographical concentration of 35 knowledge and technology-intensive industries (KTI), covering 0.43 million establishments at a district level using Economic Census (2013) data. Empirical results exhibit that the spatial dependence for high and medium-high R&D-intensive industries prevails across various districts of India. Specifically, results demonstrate that the magnitude of the geographical concentration effect differs across high and medium-high R&D-intensive industries and the high-high employment cluster, mainly perceptible in Maharashtra and Telangana states in India. Moreover, the results validate that the substantial evidence of employment concentration of KTI industries has been confined to only a few specific districts of different states in India. Further, we estimate a regression line between the unweighted and weighted Ellison-Glaeser index for a more robust analysis and to capture the neighborhood effect. Empirical results exhibit that for specific KTI industries, the estimated coefficients between these indices exceed one, indicating substantial evidence of the neighborhood effect, which facilitates the geographical concentration of a few KTI industries specific to certain locations in India. Empirical results from this study emerge specific policies to emphasize the districts to increase the employment opportunities where the KTI industry has a higher employment concentration. Further, emphasis should be given to the KTI industries to enhance their value-addition capability for various products and services.

38.

[Hybrid copper-graphene package interconnects for channel loss improvement in high-speed](#)

	<p>serial interfaces K Nagarajan, AK Vaidhyanathan, P Ramaswamy, S Kushwaha, R Sharma – Proceedings of the IEEE Electrical Design of Advanced Packaging and Systems Symposium, 2022</p> <p>Abstract: Data rates in high-speed interfaces like upcoming PCIe Gen6, SERDES, Ethernet are continuously increasing, and the design specifications are becoming more stringent to ensure required performance. Any small variation in the specifications will have significant impact on signal integrity and affect the performance. This means that the total insertion loss, ISI, non-ISI jitter in the entire interconnect should be improved. IC package plays a key role in signal integrity of the high-speed signal and there is a need to have low loss channel. Standards like PCIe have a loss requirement of 4 dB combining silicon and package, in case of non-root complex. Recent developments suggest new design trends for multi-chiplets in a single package with increasing package sizes, which can make it extremely difficult to predict insertion loss specifications. Conductivity, dielectric properties, and loss tangent drives the overall loss per unit length and the current low-loss materials have insertion loss of around 1 dB per 10 mm. While many advances have been reported in the literature, scope for improvement exists and conventional approaches of lowering DF of dielectric material or reducing the surface roughness of Copper have helped but are not adequate for the demands of high-speed interconnects. This paper proposes a novel approach by using hybrid Copper-Graphene package interconnects, which helps in reducing signal losses and improves the overall performance of the system.</p>
39.	<p>Hydrogen-induced phase stability and phonon mediated-superconductivity in two-dimensional van der Waals Ti₂C MXene monolayer P Tsuppayakorn-aek, T Bovornratanaraks, R Ahuja... - Physical Chemistry Chemical Physics, 2022</p> <p>Abstract: Herein, we report the phase stability of the hydrogenated Ti₂C MXene monolayer using an evolutionary algorithm based on density functional theory. We predict the existence of hexagonal Ti₂CH, Ti₂CH₂, and Ti₂CH₄. The dynamic and energetic stabilities of the predicted structures are verified through phonon dispersion and formation energy, respectively. The electron–phonon coupling is carefully investigated by employing isotropic Eliashberg theory. The T_c values are 0.2 K, 2.3 K, and 9.0 K for Ti₂CH, Ti₂CH₂, and Ti₂CH₄, respectively. The translation and libration adopted by stretch and bent vibrations contribute to the increasing T_c of Ti₂CH₄. The high-frequency hydrogen modes contribute to the critical temperature increase. Briefly, this work not only highlights the effect of H-content on the increments of T_c for Ti₂CH_x, but also demonstrates the first theoretical evidence of the existence of H-rich MXene in the example of Ti₂CH₄. Therefore, it potentially provides a guideline for developing hydrogenated 2D superconductive applications.</p>
40.	<p>Image super-resolution with content-aware feature processing N Mehta, S Murala - IEEE Transactions on Artificial Intelligence, 2022</p> <p>Abstract: Image super-resolution (SR) is currently a very active research topic with applications spanning from computer vision to videos and graphic industries. The top performers in SR field usually employ deep or wide convolutional neural networks (CNNs) to restore the lost textures from low-resolution images. However, most of these methods adopt pixel-shuffle, and deconvolution as their up-sampling techniques and often generate conspicuous artifacts in the reconstructed image. Additionally, the ongoing trend of directly portraying the degraded low-resolution image to high-resolution via complex deep CNNs improves the reconstruction performance, but at the cost of high computational complexity. In this work, we propose a multi-level bi-cubic up-sampler network (MBUp-Net) for reconstructing high-quality SR image with restricted number of parameters. A novel Content-Aware Feature Difference (CAFD) block is presented to reform the network by focusing on contextual information. The proposed CAFD block consists of four multi-level attention blocks for better extraction of low-level features at</p>

	<p>different scales. Furthermore, we design an innovative up-sampling layer that consistently outperforms the traditional up-sampling methods. These components collaboratively endow our proposed network with a great performance boost, helping it achieve state-of-the-art accuracy on five synthetic benchmark datasets, both qualitatively and quantitatively. In addition, a detailed ablation study has been accomplished to scrutinize the improvements obtained by different modules in the proposed method.</p>
41.	<p>Linear preservers of Hadamard circulant majorization G Kosuru, S Saha - Indian Journal of Pure and Applied Mathematics, 2022</p> <p>Abstract: In this paper, we study the Hadamard circulant majorization. Also, we derive the structure of linear preservers and strong linear preservers of this Hadamard circulant majorization.</p>
42.	<p>Loneliness and social anxiety as predictors of problematic phone use and compulsive internet use among youth of punjab P Singh, K Jain, A Singh - Psychological Studies, 2022</p> <p>Abstract: The rapid growth in the accessibility of technology mediums has resulted in the growing dependency and is associated with Compulsive Internet Use (CIU) and Problematic Phone Use (PPU). The present study was an effort to study the relationship between psychosocial problems like loneliness and social anxiety with problematic phone use (PPU) and compulsive internet use (CIU). It was hypothesized that loneliness and social anxiety would significantly PPU and CIU. A total of 260 participants (149 males and 111 females) within the age range of 17–35 years (M=23.3, SD 3.01) responded on four standardized questionnaires viz., Smartphone Addiction Scale-Short Version (Kwon et al. in PLoS ONE 8:56936, 2013), Compulsive Internet Use Scale (Meerkerk et al. in Cyberpsychol Behav 12:1–6, 2009), UCLA loneliness scale-version 3 (Russel et al. in J Personal Assess 66:20–40, 1996), and Social Anxiety Questionnaire for Adults (Caballo et al. in Behav Ther 43:313–328, 2012). The regression results showed that loneliness and social anxiety emerged to be significant predictors of Problematic Phone Use (PPU) and Compulsive Internet use (CIU). The findings and implications are discussed in the paper.</p>
43.	<p>Machine learning-based analytical systems: Food forensics Ranbir, M Kumar, G Singh, J Singh, N Kaur, N Singh - ACS Omega, 2022</p> <p>Abstract: Despite a large amount of money being spent on both food analyses and control measures, various food-borne illnesses associated with pathogens, toxins, pesticides, adulterants, colorants, and other contaminants pose a serious threat to human health, and thus food safety draws considerable attention in the modern pace of the world. The presence of various biogenic amines in processed food have been frequently considered as the primary quality parameter in order to check food freshness and spoilage of protein-rich food. Various conventional detection methods for detecting hazardous analytes including microscopy, nucleic acid, and immunoassay-based techniques have been employed; however, recently, array-based sensing strategies are becoming popular for the development of a highly accurate and precise analytical method. Array-based sensing is majorly facilitated by the advancements in multivariate analytical techniques as well as machine learning-based approaches. These techniques allow one to solve the typical problem associated with the interpretation of the complex response patterns generated in array-based strategies. Consequently, the machine learning-based neural networks enable the fast, robust, and accurate detection of analytes using sensor arrays. Thus, for commercial applications, most of the focus has shifted toward the development of analytical methods based on electrical and chemical sensor arrays. Therefore, herein, we briefly highlight and review the recently reported array-based sensor systems supported by machine learning and multivariate analytics to monitor food safety and quality in the field of food forensics.</p>



44.	<p>Machine-learning predictions of caffeine co-crystal formation accompanying experimental and molecular validations TA Syed, KB Ansari, A Banerjee, DA Wood, MS Khan... - Journal of Food Process Engineering, 2022</p> <p>Abstract: Caffeine co-crystal formation with other compounds is investigated in this study using a variety of machine learning (ML) methods. A total of 140 caffeine co-crystal data points are used to train classification learners using MATLAB ML models. Kernel neural network, ensemble tree-based, logistic regression, and support vector machine algorithms were among the ML models tested. The logistic regression algorithm produced the most accurate predictions of caffeine-co-crystal formation, with a validation accuracy of 97.1%. Experiments and molecular interaction studies between caffeine and other tea compounds (catechin and catechol) are used to validate ML predictions. As part of the evaluation, a random forest classifier was applied to select 1440 known molecular descriptors, among them 30 descriptors identified as responsible for caffeine co-crystal formation were used for training and validation purpose. The reliability of the trained logistic regression algorithm means that it is suitable for use in predicting possible co-crystals between caffeine and other compounds, thereby providing an understanding of caffeine co-crystals formation without recourse to rigorous experimental tests.</p>
45.	<p>Measurement and analysis of tool wear and surface characteristics in micro turning of SLM Ti6Al4V and wrought Ti6Al4V J Airao, H Kishore, CK Nirala - Measurement, 2023</p> <p>Abstract: Parts produced using additive manufacturing (AM) have a significant transition in the features such as surface quality, residual stresses, microhardness, etc. To make the AM component suitable for an application, post-processing of the parts is required to remove the non-desirable features. In this regard, the micro turning of selective laser melted (SLM) Ti6Al4V are conducted to examine the surface characteristics, tool wear and chip morphology. The results obtained for SLM Ti6Al4V are compared with the results of wrought Ti6Al4V. Attributed to the higher strength and hardness, the SLM Ti6Al4V shows a higher tool wear and surface roughness than the wrought Ti6Al4V. The main tool wear mechanisms involved are built-up edge formation, adhesion, abrasion, and edge chipping for both the materials. The surface roughness is found increased with increasing cutting speed and feed. The wrought Ti6Al4V shows less feed marks and chip adhesion compared to SLM Ti6Al4V. Moreover, the materials side flow is observed in SLM Ti6Al4V only. The chips produced are long and continuous for wrought Ti6Al4V, whereas they are discontinuous for SLM Ti6Al4V. Morphology of the chips shows that they are of scaly structure for SLM Ti6Al4V for all the parameters, whereas they are of lamella structure for wrought Ti6Al4V, particularly at low feed and cutting speed.</p>
46.	<p>Microwave ablation trocar operated at dual tine dual-frequency: A numerical analysis S Vellavalapalli, R Repaka - Journal of Engineering and Science in Medical Diagnostics and Therapy, 2022</p> <p>Abstract: Microwave ablation (MWA) is a minimally invasive thermal ablation technique that has the advantages of obtaining high intratumoral temperatures, less treatment time, and large ablation region as compared to other thermal ablation techniques. The ablation region obtained during MWA procedure mainly depends on the design and type of the trocar being used. The</p>

trocar plays an essential role in the MWA system by governing the energy distribution during tissue ablation. In this study, a novel MWA trocar design has been considered to achieve concentrated ablation region along the tumor's spatial distribution. A dual tine trocar with each tine supplied with energy at different frequencies (2.45 GHz and 6 GHz) has been considered for tumor ablation. Commercially available Finite Element based software has been used (comsol-multiphysics) to analyze the extent of ablation zone. Coupled bioheat and electromagnetic physics interfaces have been utilized. Results showed that the proposed trocar with tines operating at 6 GHz on both the tines leads to a large ablation region (3 cm in diameter) with spherical in shape. Irregularly shaped ablation region can also be achieved by this trocar with tines operating at different frequencies. The minimum time required for complete tumor ablation by the trocar operated at 6 GHz is 4 min, followed by 6 min for the trocar operated at 2.45 GHz. The proposed trocar can become a part of a better treatment planning system based on tumor shape, nearby blood vessel presence, and the trocar's precise insertion.

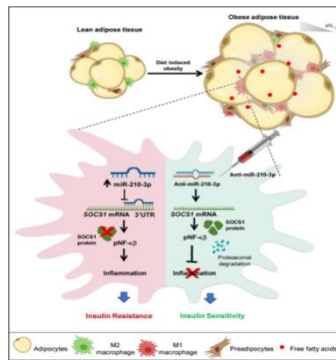
[miR-210-3p promotes obesity-induced adipose tissue inflammation and insulin resistance by targeting SOCS1 mediated NF-κB pathway](#)

D Patra, S Roy, L Arora, SW Kabeer, S Singh, U Dey...D Pal - Diabetes, 2022

47.

Abstract: Under the condition of chronic obesity, an increased level of free fatty acids along with low oxygen tension in the adipose tissue creates a pathophysiological adipose tissue microenvironment (*ATenv*) leading to the impairment of adipocyte function and insulin resistance. Here, we found the synergistic effect of hypoxia and lipid (HL) surge in fostering adipose tissue macrophages(ATMs) inflammation and its polarization. *ATenv* significantly increased *miR-210-3p* expression in ATMs which promotes NF-κB activation-dependent proinflammatory cytokines expressions along with the downregulation of anti-inflammatory cytokines expression. Interestingly, delivery of *miR-210-3p* mimic significantly increased the macrophage inflammation in absence of HL co-stimulation; while *miR-210-3p* inhibitor notably compromised HL-induced macrophage inflammation through increased production of SOCS1 (suppressor of cytokine signalling 1), a negative regulator of NF-κB inflammatory signalling pathway. Mechanistically, *miR-210* directly binds to 3' UTR of *SOCS1* mRNA and silenced its expression and thus preventing proteasomal degradation of NF-κB p65. Direct delivery of anti-*miR-210-3p* LNA in the *ATenv* markedly rescued mice from obesity-induced adipose tissue inflammation and insulin resistance. Thus, *miR-210-3p* inhibition in ATMs could serve as a novel therapeutic strategy for managing obesity-induced type 2 diabetes.

Graphical Abstract:



[Modeling permafrost distribution using geoinformatics in the alaknanda valley, uttarakhand, india](#)

48.

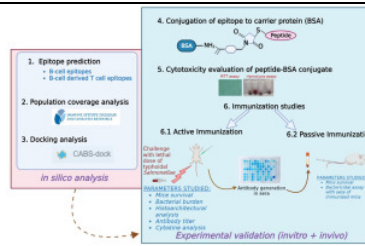
AC Pandey, T Ghosh, BR Parida, CS Dwivedi, RK Tiwari – Sustainability, 2022

Abstract: The Indian Himalayan region is experiencing frequent hazards and disasters related to

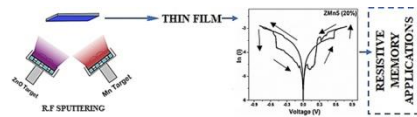
	<p>permafrost. However, research on permafrost in this region has received very little or no attention. Therefore, it is important to have knowledge about the spatial distribution and state of permafrost in the Indian Himalayas. Modern remote sensing techniques, with the help of a geographic information system (GIS), can assess permafrost at high altitudes, largely over inaccessible mountainous terrains in the Himalayas. To assess the spatial distribution of permafrost in the Alaknanda Valley of the Chamoli district of Uttarakhand state, 198 rock glaciers were mapped (183 active and 15 relict) using high-resolution satellite data available in the Google Earth database. A logistic regression model (LRM) was used to identify a relationship between the presence of permafrost at the rock glacier sites and the predictor variables, i.e., the mean annual air temperature (MAAT), the potential incoming solar radiation (PISR) during the snow-free months, and the aspect near the margins of rock glaciers. Two other LRMs were also developed using moderate-resolution imaging spectroradiometer (MODIS)-derived land surface temperature (LST) and snow cover products. The MAAT-based model produced the best results, with a classification accuracy of 92.4%, followed by the snow-cover-based model (91.9%), with the LST-based model being the least accurate (82.4%). All three models were developed to compare their accuracy in predicting permafrost distribution. The results from the MAAT-based model were validated with the global permafrost zonation index (PZI) map, which showed no significant differences. However, the predicted model exhibited an underestimation of the area underlain by permafrost in the region compared to the PZI. Identifying the spatial distribution of permafrost will help us to better understand the impact of climate change on permafrost and its related hazards and provide necessary information to decision makers to mitigate permafrost-related disasters in the high mountain regions.</p>
49.	<p>Morphed inception of dynamic Leidenfrost regime in colloidal dispersion droplets G VVS Vara Prasad, M Yadav, P Dhar, D Samanta - <i>Physics of Fluids</i>, 2022</p> <p>Abstract: Droplet impact on a heated substrate is an important area of study in spray cooling applications. On substrates significantly hotter than the saturation temperature, droplets immediately hover on its vapor cushion, exhibiting the Leidenfrost phenomenon. Here, we report the phenomena wherein addition of Al₂O₃ nanoparticles to water significantly increases the onset of dynamic Leidenfrost temperature (T_{DL}) and suppresses the overall Leidenfrost regime. We experimentally revealed that the onset of T_{DL} delays with increasing the nanoparticle concentration of the colloidal dispersions at a particular Weber number (We). But, for a constant concentration, the onset of T_{DL} decreases with an increase in impact We. In contrast to water droplets, the colloid droplets exhibit vigorous spraying behavior due to the nanoparticulate residue deposition during the spreading and retraction stages. Further, the residue on the heated substrate changes the departure diameter of the vapor bubbles during boiling, prevents bubble coalescence and vapor layer formation, and reduces the propensity to attain dynamic Leidenfrost regime. With the aid of scaling analysis of T_{DL} with impact We, we have explored the thermo-hydrodynamic behavior of impacting colloid droplets on a superheated substrate. Finally, we have also segregated the different boiling regimes of colloid droplets over various impact We.</p>
50.	<p>Neural encoding of songs is modulated by their enjoyment G Sharma...A Dhall - <i>Proceedings of the International Conference on Multimodal Interaction</i>, 2022</p> <p>Abstract: We examine user and song identification from neural (EEG) signals. Owing to perceptual subjectivity in human-media interaction, music identification from brain signals is a challenging task. We demonstrate that subjective differences in music perception aid user identification, but hinder song identification. In an attempt to address intrinsic complexities in music identification, we provide empirical evidence on the role of enjoyment in song recognition. Our findings reveal that considering song enjoyment as an additional factor can improve EEG-based song recognition.</p>
51.	<p>Optimization of wire-edm process parameters for ti6al4v alloy cutting using mayfly algorithm</p>

	<p>AK Singh, KS Bal, D Dey, AR Pal, DK Pratihar... - Advances in Modern Processes: Book Chapter, 2023</p> <p>Abstract: The present work is an extension of the work carried out by the authors previously. In the present study, the optimization of input parameters for wire-EDM cutting of a 2.5 mm thick Ti6Al4V alloy sheet was carried out to have desired cut quality and cutting speed. The experiments were statistically designed using an L8 orthogonal array. Voltage, current, capacitance, duty cycle, frequency, wire tension, and wire feed, were chosen as the input parameters. Kerf width, taper angle, surface roughness, and cutting speed were considered as the outputs. A newly developed, nature-inspired algorithm, called the Mayfly optimization algorithm, was used to minimize the kerf width, taper angle, and surface roughness, along with maximization of cutting speed. The minimum value of current, duty cycle, and frequency were found to be favorable to predict the desired output due to lower spark-energy generation. At the same time, the maximum value of voltage, wire feed, and wire tension were formulated by the algorithm for obtaining desired output. Upon confirmation test using the optimized process parameters, satisfactory experimental results were found for the predicted results within acceptable error.</p>
52.	<p>Photoredox catalyzed single c–f bond activation of trifluoromethyl ketones: A solvent controlled divergent access of gem-difluoromethylene containing scaffolds S Ghosh, ZW Qu, S Roy, S Grimme, I Chatterjee - Chemistry–A European Journal, 2022</p> <p>Abstract: Selective defluorinative functionalization of trifluoromethyl ketones is a long-standing challenge owing to the exhaustive mode of the process. To meet the demands for the installation of the gem-difluoromethylene unit for the construction of the molecular architectures of well-known pharmaceuticals and agrochemicals, a distinct pathway is thereby highly desirable. Here, we introduce a protocol that allows the divergent synthesis of gem-difluoromethylene group containing tetrahydrofuran derivatives and linear ketones via single C–F bond activation of trifluoromethyl ketones using visible-light photoredox catalysis in the presence of suitable olefins as trapping partner. The choice of appropriate solvent and catalyst plays a significant role in controlling the divergent behavior of this protocol. Highly reducing photo-excited catalysts are found to be responsible for the generation of α,α-difluoromethyl ketone (DFMK) radicals as the key intermediate via a SET process. This protocol also results in a high diastereoselectivity towards the formation of partially fluorinated cyclic ketal derivatives with simultaneous construction of one C–C and two C–O bonds. State-of-the-art DFT calculations are performed to address the origin of diastereoselectivity as well as the divergence of this protocol.</p>
53.	<p>Physiological sensing for media perception & activity recognition G Sharma - Proceedings of the International Conference on Multimodal Interaction, 2022</p> <p>Abstract: Wearable sensors have the intriguing potential to continuously evaluate human physiological characteristics in real-time without being obtrusive. This thesis aims to incorporate physiological sensors data to investigate the Media Perception and Activity Recognition. Our primary research goals include (a) neural encoding-based psycho-acoustic attribute analysis for data sonification, (b) empirical evidence for perceptual subjectivity in neural encoding during human-media interactions, the impact of incorporating behavioral ratings, and (c) the efficacy of attention-based transformer models on physiological data on human activity recognition problems.</p>
54.	<p>Plasmonic response of metallic nanoparticles embedded in glass and a-Si GP Singh, N Sardana - Bulletin of Materials Science, 2022</p> <p>Abstract: The optical properties of nanoparticle (NP) metals displaying the highest plasmonic response (silver, gold, copper and aluminium) are simulated. Embedding the metal NPs in a dielectric medium provides prevention from agglomeration, increased absorption and protection</p>

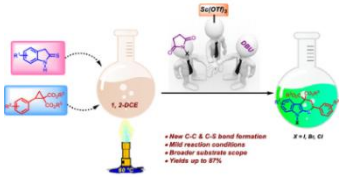
	<p>from environmental effects. Hence, embedding is an effective method to improve the performance of plasmonic-based devices. The NPs of the aforementioned metals were simulated in air, glass and a-Si environment from the ultraviolet to the near-infrared range. Spheres, nanobars and nanoprisms of volume equal to spheres of diameter 50–200 nm were studied in a broad wavelength range of 200–1800 nm. The effect of the material, size, shape and environment was observed quantitatively by analysing the peak shifts of the dipole and higher-order poles. The highest extent of peak shift due to change in size and surrounding environment was for aluminium, followed by silver, gold and copper.</p>
55.	<p>Polymer-derived microporous SiOC ceramic coated gallium nitride sensor for selective H₂/CO detection B Kumar, RM Prasad - <i>Sensors and Actuators B: Chemical</i>, 2022</p> <p>Abstract: In this work enhancement of H₂/CO selectivity of GaN sensors coated with amorphous microporous silicon oxycarbide (SiOC) filter layer has been studied. Amorphous SiOC ceramic has been synthesized by pyrolysis of vinyl-functionalized polysiloxane at 700 °C under argon. N₂-adsorption measurement confirms formation of microporous SiOC ceramic. SiOC layer with a thickness of about 6 μm was coated on GaN sensor substrate after two-fold coating/pyrolysis steps. Transient response characteristics and sensor signals of uncoated GaN and SiOC-coated GaN sensors were measured towards H₂ (50, 500 and 1000 ppm) and CO (50, 70 and 100 ppm) in nitrogen at 400 °C. Uncoated GaN showed high sensor signal towards both H₂ and CO whereas for SiOC-coated GaN almost no sensing towards CO was found.</p>
56.	<p>Potential of a novel flagellin epitope as a broad-spectrum vaccine candidate against enteric fever S Vij, R Thakur, L Kumari, CR Suri, P Rishi - <i>Microbial Pathogenesis</i>, 2023</p> <p>Abstract: Relentless emergence of antibiotic resistant Salmonella strains, coupled with the drawbacks associated with currently available vaccines against enteric fever, warrants an urgent need to look for new vaccine candidates. Out of the multiple virulence factors harbored by Salmonella, flagella are regarded as one of the most important targets of innate as well as adaptive immune response. Individual Salmonella serotypes alternate between expression of two different antigenic forms encoded by fliC and fljB genes, respectively thereby employing this as a strategy to escape the host immune response. In the present study, using various immunoinformatic approaches, a flagellin epitope, present in both antigenic forms of typhoidal Salmonellae has been targeted. Following B-cell epitope and B-cell derived T-cell epitope prediction and interaction studies with major histocompatibility complexes using molecular docking, a peptide epitope was selected. Further, it was screened for its presence in majority of typhoidal serovars along with other useful attributes, in silico. Thereafter, safety studies were performed with the synthesized peptide. Subsequently, immunization studies were carried out using S. Typhi as well as S. Paratyphi A induced murine peritonitis model. Active immunization with peptide-BSA conjugate resulted in 75% and 80% mice survival following lethal challenge with S. Typhi and S. Paratyphi A respectively, along with a significant IgG antibody titer, thereby highlighting its immunogenic potential. Reduced bacterial burden in vital organs along with improved histoarchitecture and cytokine levels further substantiated the protective efficacy of the proposed candidate. Passive immunization studies with the candidate verified the protective efficacy of the generated antibodies against lethal challenge of bacteria in mice. Given the endemic nature of enteric fever and the antigenic variability observed in Salmonella serotypes, present study highlights the importance of using a vaccine candidate, which, along with generating a strong immune response, also exhibits a broad coverage against both, S. Typhi as well as S. Paratyphi A strains.</p> <p>Graphical Abstract:</p>



57.	<p>Process competencies of modulation-assisted machining M Singh, S Dhiman, H Singh, CC Berndt - <i>Advances in Modern Machining Processes: Lecture Notes in Mechanical Engineering Book Series</i>, 2023</p> <p>Abstract: With the development of new materials with enhanced mechanical properties, there is a parallel requirement for advanced machining processes. Materials including titanium alloys and nickel superalloys are widely used in the aerospace industry due to their high strength-to-weight ratio and are classified as difficult-to-machine materials. It is challenging to machine this class of materials with conventional machining processes. Thus, advanced machining processes, like modulation-assisted machining (MAM), can be a better alternative. In light of the same, this paper provides a review of process capabilities of MAM processes. Moreover, this paper provides a quantitative comparison of MAM with its conventional counterpart. Studies by various authors have been discussed and it was concluded that MAM is a promising contender for machining difficult-to-machine materials.</p>
58.	<p>Putative targeting by BX795 causes decrease in protein kinase C protein levels and inhibition of HSV1 infection RK Suryawanshi, CD Patil, D Wu, PK Panda, SK Singh, I Volety, R Ahuja... - <i>Antiviral Research</i>, 2022</p> <p>Abstract: Herpes simplex virus type-1 (HSV1) exploits cellular machinery for its own replicative advantage. Current treatment modalities against HSV1 cause toxicity and drug resistance issues. In the search for alternative forms of treatment, we have uncovered a small molecule, BX795, as a candidate drug with strong antiviral potential owing to its multitargeted mode of action. In this study, we show that in addition to a previously known mechanism of action, BX795 can directly interact with the proviral host factor protein kinase C (PKC) in silico. When administered to HSV1 or mock infected human corneal epithelial (HCE) cells, BX795 significantly reduces the protein level and perinuclear localization of proviral PKC-α and PKC-ζ isoforms. This activity closely mimics that of a known PKC inhibitor, Bisindolylmaleimide I (BIM I), which also inhibits viral replication. Taken together our studies demonstrate a previously unknown mechanism by which BX795 exerts its antiviral potential.</p>
59.	<p>Quantum synchronization and entanglement of indirectly coupled mechanical oscillators in cavity optomechanics: A numerical study D Garg, Manju, S Dasgupta, A Biswas - <i>Physics Letters A</i>, 2022</p> <p>Abstract: It is often conjectured that quantum synchronisation and entanglement are two independent properties which two coupled quantum systems may not exhibit at the same time. However, as both these properties can be understood in terms of the second order moments of a set of conjugate quadratures, there may exist specific conditions for simultaneous existence of entanglement and quantum synchronization. Here we present a theoretical scheme to achieve the same between two mechanical oscillators, which are indirectly coupled with each other via a coupling between two cavities. We show that in the presence of the cavity-oscillator coupling, quadratically varying with their displacements, these oscillators can be synchronized in the quantum sense and entangled as well, at times much longer than the decay time-scale of the cavity modes. Precisely speaking, we show that in the presence of quadratic coupling,</p>

	<p>entanglement criterion and quantum synchronization measure are simultaneously satisfied in steady state. This behaviour can be observed for a range of quadratic coupling, temperature, and frequency difference of the two oscillators.</p>
60.	<p>Smoothed floating node method for modelling cohesive fracture in quasi-brittle materials U Singh, S Kumar - Mechanics of Advanced Materials and Structures, 2022</p> <p>Abstract: This paper presents a numerical framework for implementation of cohesive zone model with smoothed floating node method (SFNM) for failure analysis of quasi-brittle materials. The nonlinear behavior of material inside the fracture process zone in front of the crack tip is modeled with a potential-based intrinsic cohesive zone approach. Here, SFNM is used to represent the kinematics of crack and the crack front inside the domain without the requirement of remeshing and discontinuous enrichment functions during crack growth, hence resolves the issues associated with the existing discrete numerical methods. A strain smoothing technique is adopted over the domain through which classical domain integration changes to line integration along each boundary of the smoothing cell, hence derivative of shape functions are not required in the computation of the field gradients, thus resolves the issue of element distortion. The proposed numerical framework is firstly verified using the patch test of the two-dimensional specimen under mode I and mode II loading conditions and subsequently extended for solving the two-dimensional standard fracture problems. The effectiveness of the proposed framework is checked by comparing the computational results with the available literature results.</p>
61.	<p>Sputter deposited mn-doped zno thin film for resistive memory applications AK Chawla, R Jain, J Singh, KH Mir, T Garg, AU Rao...N Sardana... - ChemistrySelect, 2022</p> <p>Abstract: Transition metal doped Zinc oxide (ZnO) thin films with wide band gap semiconducting nature have diverse range of applications including, gas sensors, optical and optoelectronic devices, electronics and spintronics spintronic devices etc. In the present study, Manganese (Mn)-doped ZnO thin films deposited on glass substrates using RF-magnetron sputtering have been investigated for their optical and electrical behavior aiming at resistive random access memory applications. To study the influence of Mn doping and correlation between the structural and the physical properties of the films, the samples were characterized by X-ray Diffraction (XRD), Raman spectroscopy, Field Emission Scanning Electron Microscopy (FESEM), Energy Dispersive X-ray Spectroscopy (EDS), UV-VIS spectrophotometry and X-ray photoelectron spectroscopy (XPS). The films are found to be crystalline and a decrease in lattice parameter from 2.6049 Å to 2.5845 Å, an increase in optical band gap from 3.27 eV to 3.35 eV and a decrease in Urbach energy from 0.222 eV to 0.171 eV, is observed with increase in Mn-concentration. The electrical performance of the film with highest Mn-content is found to be more suitable for resistive memory applications. Tailoring the electrical behavior of the film by incorporating Mn as dopant is an important approach to find suitable material combination for novel memory devices.</p> <p>Graphical Abstract: The work describes the synthesis of Mn doped ZnO by RF- magnetron sputtering for resistive memory application. The structure of film are discussed based on XRD, Raman Spectroscopy and XPS. Band gap of film are determined by UV spectroscopy. Surface morphology are conversed by FESEM.</p> 
62.	<p>Stability of and conduction in single-walled Si₂ BN nanotubes D Singh, V Shukla...R Ahuja - Physical Review Materials, 2023</p>

	<p>Abstract: We explore the possibility and potential benefit of rolling a Si₂BN sheet into single-walled nanotubes (NTs). Using density functional theory (DFT), we consider both structural stability and the impact on the nature of chemical bonding and conduction. The structure is similar to carbon NTs and hexagonal boron-nitride (hBN) NTs and we consider both armchair and zigzag Si₂BN configurations with varying diameters. The stability of these Si₂BN NTs is confirmed by first-principles molecular dynamics calculations, by exothermal formation, an absence of imaginary modes in the phonon spectra. Also, we find the nature of conduction varies from semiconducting over semimetallic to metallic, reflecting differences in armchair/zigzag-type structures, curvature effects, and the effect of quantum confinement. We present a detailed characterization of how these properties lead to differences in both the bonding nature and electronic structures.</p>
63.	<p>Stationary black holes and stars in the Brans-Dicke theory with $\Lambda > 0$ revisited MS Ali, S Bhattacharya, S Kaushal - Physical Review D, 2022</p> <p>Abstract: It was shown a few years back that for a stationary regular black hole or star solution in the Brans-Dicke theory with a positive cosmological constant Λ, endowed with a de Sitter or cosmological event horizon in the asymptotic region, not only there exists no nontrivial field configurations, but also the inverse Brans-Dicke parameter $\omega-1$ must be vanishing. This essentially reduces the theory to Einstein's general relativity. The assumption of the existence of the cosmological horizon was crucial for this proof. However, since the Brans-Dicke field ϕ, couples directly to the Λ-term in the energy-momentum tensor as well as Λ acts as a source in ϕ's equation of motion, it seems reasonable to ask: can ϕ become strong instead and screen the effect of Λ, at very large scales, so that the asymptotic de Sitter structure is replaced by some alternative, yet still acceptable boundary condition? In this work we analytically argue that no such alternative exists, as long as the spacetime is assumed to be free of any naked curvature singularity. We further support this result by providing explicit numerical computations. Thus we conclude that in the presence of a positive Λ, irrespective of whether the asymptotic de Sitter boundary condition is imposed or not, a regular stationary black hole or even a star solution in the Brans-Dicke theory always necessitates $\omega-1=0$, and thereby reducing the theory to general relativity. The qualitative differences of this result with that of the standard no hair theorems are also pointed out.</p>
64.	<p>Structure-induced tunable multipolar moments and the associated Purcell enhancement in silicon-like metasurfaces M Khokhar, FA Inam, RV Nair - Physica status solidi, 2022</p> <p>Abstract: The recent breakthrough in integrating single quantum emitters to dielectric metasurfaces opens up avenues in quantum technologies with the possibility to obtain on-demand single photon sources and efficient spin-photon interface. All-dielectric metasurfaces with unprecedented possibilities of generating directional light scattering instigated a novel concept of the Kerker effect that led to applications in nanophotonics. Here, an all-dielectric metasurface consisting of silicon-like nanodisks with square lattice symmetry that exhibits Kerker condition governed by constructive interference of multipoles optimized for the zero-phonon line (ZPL) of negatively charged nitrogen-vacancy (NV-) center at a wavelength of 640 nm is discussed. The phase and amplitude of excited multipolar moments are manipulated by varying the geometrical parameters of the metasurfaces. The constructive interference between multipolar moments generates a Kerker condition, which is tunable by varying the diameter, thickness, refractive index of nanodisks, and substrate refractive index. The Kerker condition is further used to control the emission from a single NV- center and a Purcell enhancement of 300 times is achieved at 640 nm. The study profoundly explores new insights into quantum metasurfaces and paves a new way to utilize dielectric resonators with emitters as on-chip quantum light sources at Kerker condition.</p>

65.	<p>Synthesis of indole-fused dihydrothiopyrano scaffolds via(3+3)-annulations of donor–acceptor cyclopropanes with indoline-2-thiones B Gopal, PR Singh, M Kumar, A Goswami - <i>The Journal of Organic Chemistry</i>, 2022</p> <p>Abstract: A new methodology for the synthesis of N-haloindole-fused dihydrothiopyrano derivatives via (3 + 3)-annulation of donor–acceptor cyclopropanes (DACs) with indoline-2-thiones in the presence of Sc(OTf)₃ as a Lewis acid catalyst has been developed. This protocol provides a variety of indole-fused dihydrothiopyrano molecules in good to excellent yields, which architecturally resemble other indole-fused tricyclic molecules having potential medicinal value. In addition, we have described a detailed reaction mechanism and transformation of the furnished product into N-fused thiazino indole molecule.</p> 
66.	<p>Testing policy effectiveness during COVID-19: An NK-DSGE analysis SA Shah, B Garg - <i>Journal of Asian Economics</i>, 2023</p> <p>Abstract: We examine the effectiveness of fiscal and monetary policy in mitigating the impact of COVID-19 in India using the NK-DSGE framework. In terms of policy effectiveness, our findings imply that expansionary monetary policy is effective in reviving economic growth both from the demand side and supply side. In contrast, expansionary fiscal policy is effective only from the supply side. Our findings recommend the implementation of optimal policy mix in a coordinated and staggered framework for effective mitigation of ill-effects of the COVID-19, such as reviving employment and capacity utilization to its pre-pandemic level with minimal inflationary effects.</p>
67.	<p>The multiscale characterization and constitutive modeling of healthy and type 2 diabetes mellitus Sprague Dawley rat skin KK Dwivedi, P Lakhani, P Sihota, K Tikoo, S Kumar, N Kumar - <i>Acta Biomaterialia</i>, 2022</p> <p>Abstract: In type 2 diabetes mellitus (T2DM), elevated glucose level impairs the biochemistry of the skin which may result in alteration of its mechanical and structural properties. The several aspects of structural and mechanical changes in skin due to T2DM remain poorly understood. To fill these research gaps, we developed a non-obese T2DM rat (Sprague Dawley (SD)) model for investigating the effect of T2DM on the <i>in vivo</i> strain stress state, mechanical and structural properties of skin. <i>In vivo</i> strain and mechanical anisotropy of healthy and T2DM skin were measured using the digital imaging correlation (DIC) technique and DIC coupled bulge experiment, respectively. Fluorescence microscopy and histology were used to assess the collagen and elastin fibers microstructure whereas nanoscale structure was captured through atomic force microscopy (AFM). Based on the microstructural observations, skin was modeled as a multilayer membrane where in and out of plane distribution of collagen fibers and planar distribution of elastin fibers were cast in constitutive model. Further, the state of <i>in vivo</i> stresses of healthy and T2DM were measured using model parameters and <i>in vivo</i> strain in the constitutive model. The results showed that T2DM causes significant loss in <i>in vivo</i> stresses ($p < 0.01$) and increase in anisotropy ($p < 0.001$) of skin. These changes were found in good correlation with T2DM associated alteration in skin microstructure. Statistical analysis emphasized that increase in blood glucose concentration (HbA1c) was the main cause of impaired biomechanical properties of skin. The presented data in this study can help to understand the skin pathology and to simulate the skin related clinical procedures.</p>

68.	<p>Theoretical investigation of interacting molecular motors A Jindal, T Midha, AK Gupta - <i>Nonlinear Dynamics of Nanobiophysics: Book Chapter, 2022</i></p> <p>Abstract: The transportation of matter, energy, and information is a crucial requirement for the functioning of any complex system ranging from biological to physical processes. Within a living cell, the efficient delivery of proteins to various parts (intracellular transport) is of fundamental importance to normal cellular function and development.</p>
69.	<p>Thermodynamics analysis of a novel absorption heat transformer-driven combined refrigeration and desalination system R Beniwal, K Garg, H Tyagi - <i>Energy Conversion and Management, 2023</i></p> <p>Abstract: Preservation of food and medicines below sub-zero temperatures is the need of the present times. To achieve the required temperature using renewable energy, a waste heat-driven vapour absorption refrigeration system can be implemented. Majority of the available waste heat is available in the low temperature range i.e. between 60–80 °C, which cannot be directly used to provide refrigeration. Therefore, an absorption heat transformer (AHT) is coupled with the VARS (Vapour absorption refrigeration system) system which increases temperature of this waste heat, and the upgraded heat is utilized to produce required refrigeration effect. Further, the rectifiers' waste heat of the absorption system will be used to power humidification-dehumidification (HDH) desalination cycle. Although all these three components (AHT, VARS, and HDH) have been studied individually, but they have never been combined altogether. This paper presents a mathematical model for the proposed system and its validation against published available literature. The performance parameters such as coefficient of performance, gain output ratio and refrigeration effect of the system is evaluated at different evaporator and desorber temperatures. For 300 kW waste heat at 80 °C, evaporator (VARS) temperature of –10 °C, the system reported 70 kW of refrigeration effect is provided with 20 kg/hr of distillate production rate. An exergy destruction of 82.64 kW has been reported for total input exergy of 142.2 kW, for refrigeration capacity of 157 kW.</p> <p>Graphical Abstract:</p>
70.	<p>Tipping points in spatial ecosystems driven by short-range correlated noise K Pal, S Deb, PS Dutta - <i>Physical Review E, 2022</i></p> <p>Abstract: Complex spatial systems can experience critical transitions or tipplings on crossing a threshold value in their response to stochastic perturbations. While previous studies have well characterized the impact of white noise on tipping, the effect of correlated noise in spatial ecosystems remains largely unexplored. Here, we investigate the effect of both multiplicative and additive Ornstein-Uhlenbeck (OU) correlated noise on the occurrence of critical transitions in spatial ecosystems. We find that decreasing the noise correlation time of OU (exponentially correlated) noise aggravates the chance of critical transitions in spatiotemporal ecological systems. Our results hold good and are supported by the analysis of three well-studied spatial</p>

	<p>ecological models of varying nonlinearity. We also compute spatial early warning indicators (e.g., spatial variance, spatial skewness, and spatial correlation) to determine their reliability in anticipating tipping points with variations in noise correlation. The indicators of critical transitions exhibit mixed success in forewarning the occurrence of a tipping point, as indicated by the distribution of Kendall's rank correlation.</p>
71.	<p>Unified multi-weather visibility restoration A Kulkarni, PW Patil, S Murala, S Gupta - IEEE Transactions on Multimedia, 2022</p> <p>Abstract: Automated surveillance is widely opted for applications such as traffic monitoring, vehicle identification, etc . But, various weather degradation factors such as rain and snow streaks, along with atmospheric veil severely affect the perceptual quality of an image, eventually affecting the performance of these applications. There exist weather specific (rain, haze, snow, etc .) methods focusing on respective restoration task. As image restoration is a preprocessing step for high level surveillance applications, it is practically inapplicable to have different architectures for different weather restoration. In this paper, we propose a lightweight unified network, having 1.1M parameters (1 / 40 th and 1 / 6 th of the existing state-of-the-art rain with veil removal, and snow with veil removal methods respectively) for removal of rain and snow along with the veiling effect present in the images. In this network, we propose two parallel streams to handle the degradations and restoration: First, degradation removal stream (DRS) focuses mainly on removing randomly repeating degradations i.e., rain and snow streaks, through the proposed adaptive multi-scale feature sharing block (AMFSB) and stage-wise subtractive block (SSB). Second, feature corrector stream (FCS) mainly focuses on refining the partial outputs of the first stream, reducing the veiling effect and acts supplementary to the first stream. Finally, we leverage contrastive regularization for better convergence of the proposed network. Substantial experiments on synthetic as well as real-world images, along with extensive ablation studies, demonstrate that the proposed method performs competitively with the existing state-of-the-art methods for multi-weather image restoration. The code is available at: https://github.com/AshutoshKulkarni4998/UVRNet .</p>
72.	<p>Viscoelastic properties of osteoarthritic human knee articular cartilage JA Gaonkar, R Kumar - Eurasia Conference on Biomedical Engineering, Healthcare and Sustainability, 2022</p> <p>Abstract: The musculoskeletal system relies heavily on articular cartilage, which is a hydrated supportive tissue that covers diarthrodial joints. Most people over the age of 55 suffer from osteoarthritis, which is the most common degenerative joint disease. The mechanical flexibility, lubricating behaviour, damping function, and energy absorption and dissipation capacity of articular cartilage - all are affected due to the osteoarthritic disorder. The changes in biomechanical viscoelastic properties of knee articular cartilage due to progression of osteoarthritis were analysed. Static deformation was imposed on low grade and high-grade osteoarthritic articular cartilage. After imposing the constant compressive stress on articular surface of the cartilage section, the time dependent stress relaxation data were acquired from the degenerated osteoarthritic tissue. An empirical model - the generalized Maxwell model - was used to analyse the changes in viscoelastic properties of osteoarthritic cartilage. The viscoelastic properties such as stress relaxation time and elastic modulus parameters of low grade and high grade osteoarthritic articular cartilage were compared and observed to differ significantly. Moreover, the mean value of instantaneous and equilibrium modulus both were observed higher in the low grade of osteoarthritic cartilage. The present results obtained using the generalized Maxwell model demonstrated that the significant changes occur in viscoelastic stress relaxation properties of knee articular cartilage during the progression of osteoarthritis. Such changes might play a crucial role in the physiological stress distribution, pathogenesis of osteoarthritic disorder and thus can ultimately affect the biomechanics of the knee joint.</p>

Disclaimer: This publication digest may not contain all the papers published. Library has compiled the publication data as per the alerts received from Scopus and Google Scholar for the affiliation “Indian Institute of Technology Ropar” for the month of December 2022. The author(s) are requested to share their missing paper(s) details if any, for the inclusion in the next publication digest.